Table 1 Comparison of calculated and JANAF tabulated formation functions for acetylene

	$\Delta_f H^0$, kJ/mole		$\Delta_f G^0$, kJ/mole		$\log K_f$	
T, K	Tabulated	Corrected	Tabulated	Corrected	Tabulated	Corrected
298.15	226.73	226.73	248.16	209.20	−43.48	−36.65
500	220.35	226.23	264.44	197.45	−27.62	−20.63
1000	202.99	223.67	315.14	169.61	−16.46	−8.86
2000	166.98	219.93	441.08	117.19	−11.52	−3.06
3000	128.29	217.02	586.35	66.42	−10.21	−1.16

culated values. Figures 2 and 3 show similar comparisons for the Gibbs energy of formation and the equilibrium constant of formation, respectively. The tabulated values of the formation functions are in obvious disagreement with values calculated using the tabulated thermal functions, indicating a lack of internal consistency in the JANAF tables. The calculated values presented here are in agreement with others in the literature.[2,3] Reference 3 is a previous version of the JANAF tables. As an additional check of the method of calculation, formation functions for methane (CH_4) and ethylene (C_2H_4) were calculated and found to agree precisely with the tabulated values.

Moreover, the tabulated and calculated values of the enthalpy of formation for acetylene are seen in Fig. 1 to agree precisely at 298.15 K. This seemed to indicate a systematic error in the tabulated values for acetylene rather than a random error or an error in method. By definition, the enthalpies of the reference elements are zero at 298.15 K. Therefore, regardless of the stoichiometric coefficients on the right side of Eq. (6), the correct value of the enthalpy of formation is calculated at 298.15 K. Intuitively, one might then suspect an error was made when writing Eq. (6) for the JANAF tables. Indeed, if Eq. (6) is written with the incorrect coefficient for H_2 as

$$C_2H_2 = 2C_{gr} + 2H_2 \tag{7}$$

and the formation functions are calculated on this basis, then the tabulated values are obtained precisely. Therefore, it is concluded that the JANAF tabulated values were incorrectly obtained using Eq. (7) as the formation reaction. The incorrect and corrected values for the thermodynamic formation functions are listed in Table 1 for a limited number of temperatures. The authors of Ref. 1 are aware of the error and plan to publish an addendum. The intent of this Note is to communicate the corrected values to the technical community as quickly as possible.

Summary

An error is found in the thermodynamic formation functions for acetylene presented in the third edition of the JANAF tables. The error is due to the use of an incorrect formation reaction for acetylene. Corrected values are given in both graphical and tabular form. The corrected functions are also available in digital form from the author.

References

[1]Chase, M. W., Jr., Davies, C. A., Downey, J. R., Jr., Frurip, D. J., Mcdonald, R. A., and Syverud, A. N., *JANAF Thermochemical Tables*, 3rd ed., Vol. 1; see also *Journal of Physical and Chemical Reference Data*, Vol. 14, 1985, Supplement 1, American Inst. of Physics, New York, 1986, pp. 3–20 and 660.

[2]Modell, M., and Reid, R. C., *Thermodynamics and its Applications*, 2nd ed., Prentice-Hall, Englewood Cliffs, 1983, pp. 334, 335.

[3]Stull, D. R., and Prophet, H., *JANAF Thermochemical Tables*, 2nd ed., National Standard Reference Data System, National Bureau of Standards, NSRDS-NBS-37, 1971.

Numerical Study of Turbulent Offset Jets with Entrainment Boundary

Yue-Tzu Yang* and Yun-Yeu Yeh†
National Cheng-Kung University, Tainan, Taiwan, Republic of China

I. Introduction

THE turbulent offset jets find many important industrial applications, such as heat exchangers, environment discharges, fluid injection systems, combustion chambers, air conditions for large buildings, etc. The flow pattern of turbulent offset jets can be divided into three characteristic regions: 1) the recirculation region, 2) the impingement region, and 3) the wall jet region, as shown in Fig. 1. The flow characteristics of turbulent offset jets were studied most recently by Pelfrey and Liburdy,[1-3] Bourque and Newman,[4] and Sawyer.[5,6]

Although many investigators have studied backward-facing step flow, only a few of the offset jets are considered, especially with entrainment boundary. In this Note, the high Reynolds form of the k-ε turbulence model and wall function for the near-wall turbulence behavior are incorporated to predict the mean flow characteristics of the flowfield at the single exit Reynolds number $Re = 15{,}000$ and different offset ratio $OR = 3, 7, 11$. The computed results are compared with the experimental data reported in the literature.

II. Mathematical Formulation

The steady conservation equations for incompressible two-dimensional Cartesian coordinates mean flow characteristics of turbulent flow can be written as

$$\frac{\partial}{\partial x}(\rho u \phi) + \frac{\partial}{\partial y}(\rho v \phi) = \frac{\partial}{\partial x}\left[\Gamma_\phi \frac{\partial \phi}{\partial x}\right] + \frac{\partial}{\partial y}\left[\Gamma_\phi \frac{\partial \phi}{\partial y}\right] + S_\phi \tag{1}$$

where ϕ stands for the dependent variables u, v, k, and ε; u and v are the local time-averaged velocity in x and y directions, respectively; and Γ_ϕ and S_ϕ are the corresponding turbulent diffusion coefficient and source term, respectively, for general variable ϕ. These equations are summarized in Table 1. The turbulent viscosity μ_t can be written as

$$\mu_t = \rho C\mu(k^2/\varepsilon) \tag{2}$$

Received July 23, 1992; revision received May 26, 1993; accepted for publication May 26, 1993.

*Associate Professor, Department of Mechanical Engineering.
†Graduate Student, Department of Mechanical Engineering.

the effective viscosity μ_e can be written as

$$\mu_e = \mu_1 + \mu_t = \mu_1 + \rho C\mu(k^2/\varepsilon) \tag{3}$$

The constants of the k-ε turbulence model suggested by Launder and Spalding[7] are shown in Table 2.

The boundary conditions used for the offset jet are shown in Fig. 2. For this flowfield a nonuniform staggered grid system with finer grids near the wall and jet exit is used.

A. Inlet Boundary (BC)

In this study, a uniform velocity profile is considered and the conditions at the exit of the nozzle are given as

$$\begin{aligned} U &= U_{in} \\ k &= k_{in} = iU_{in}^2 \\ \varepsilon &= \varepsilon_{in} = \frac{k_{in}^{3/2}}{\lambda t} \end{aligned} \tag{4}$$

where i is the turbulence intensity, λ is the length-scale constant, and t is the thickness of nozzle.

Table 1 Conservation equations

$$\frac{\partial}{\partial x}(\rho u\phi) + \frac{\partial}{\partial y}(\rho v\phi) = \frac{\partial}{\partial x}\left[\Gamma_\phi \frac{\partial \phi}{\partial x}\right] + \frac{\partial}{\partial y}\left[\Gamma_\phi \frac{\partial \phi}{\partial y}\right] + S_\phi$$

Equation	ϕ	Γ_ϕ	S_ϕ
Mass	1	0	0
x Momentum	u	μ_e	$-\frac{\partial p}{\partial x} + \frac{\partial}{\partial x}\left[\mu_e \frac{\partial u}{\partial x}\right] + \frac{\partial}{\partial y}\left[\mu_e \frac{\partial v}{\partial x}\right]$
y Momentum	v	μ_e	$-\frac{\partial p}{\partial y} + \frac{\partial}{\partial x}\left[\mu_e \frac{\partial u}{\partial y}\right] + \frac{\partial}{\partial y}\left[\mu_e \frac{\partial v}{\partial y}\right]$
Turbulence kinetic energy	k	(μ_e/σ_k)	$G - \rho\varepsilon$
Turbulence energy dissipation rate	ε	$(\mu_e/\sigma_\varepsilon)$	$\frac{\varepsilon}{k}(C_1 G - C_2\rho\varepsilon)$

Note: $G = \mu_t \left\{ 2\left[\left(\frac{\partial u}{\partial x}\right)^2 + \left(\frac{\partial v}{\partial y}\right)^2\right] + \left(\frac{\partial u}{\partial y} + \frac{\partial v}{\partial x}\right)^2 \right\}$.

Table 2 Constants of the k-ε model

C_μ	C_1	C_2	σ_k	$\sigma\varepsilon$
0.09	1.44	1.92	1.0	1.3

B. Wall Boundary (AF, AB, CD)

Due to the no-slip condition at the wall, the gradients of the flow properties are steep and have the effects of low Reynolds number phenomena. In order to simplify the problem, a finer grid distribution is considered and the wall function model is employed. The model used here is the one proposed by Launder and Spalding.[7] It can be written as

$$\frac{U_p}{(\tau_w/\rho)} C\mu^{1/4} k_p^{1/2} = \frac{1}{k} \ln\left[E y_p \frac{(C\mu^{1/2} k_p)^{1/2}}{\nu}\right] \tag{5}$$

$$\varepsilon_p = \frac{k_p^{3/2} C\mu^{3/4}}{\kappa y_p} \tag{6}$$

where U_p, y_p, k_p, and ε_p represent the velocity, normal distance, kinetic energy, and energy dissipation rate at point P near the wall. τ_w is the wall shear stress. E and κ are constants with the values of 9.0 and 0.42, respectively, according to the logarithmic law of the wall.

C. Entrainment Boundary (DE)

Along this boundary, fluid enters the solution domain at an unknown rate. However, when the boundary is far enough away from the flow region, the velocity gradients normal to the boundary can be considered as zero:

$$\frac{\partial u}{\partial y} = 0 \qquad \frac{\partial v}{\partial y} = 0 \tag{7}$$

D. Outlet Boundary (EF)

A zero gradient condition as below:

$$\frac{\partial u}{\partial x} = 0 \qquad \frac{\partial v}{\partial x} = 0 \tag{8}$$

is employed across the outlet boundary (EF). Although this boundary condition is strictly valid, only when the flow is fully developed, it is also permissible for sufficient far downstream from the region of interest.

III. Numerical Procedure

The numerical method used in the present study is based on the SIMPLE algorithm of Patankar and Spalding.[8] The conservation equations are discretized by control volume based finite difference method with power law scheme. The set of difference equations are solved iteratively using a line by line solution method in conjunction with a tridiagonal matrix form. The computation domain considered in this study extended to $x/t = 45$ and $y/t = 18$. Based on the grid independence study, 48 grid lines were used in the streamwise direction and

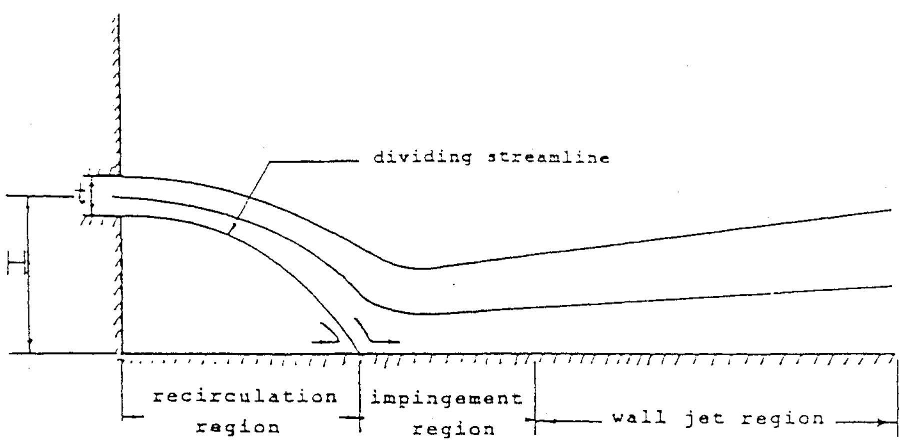

Fig. 1 Offset jet flow geometry.

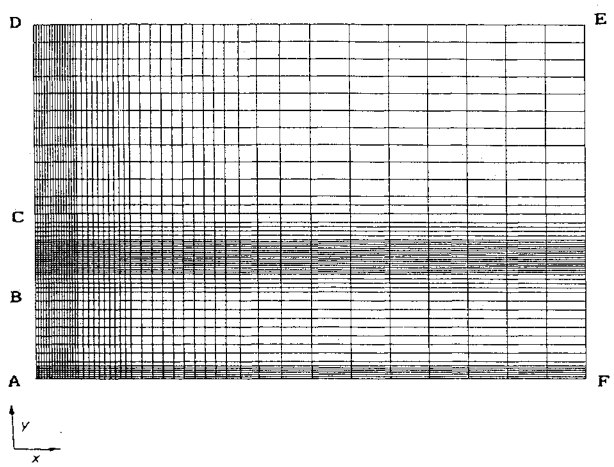

Fig. 2 **Boundary conditions for computing domain.**

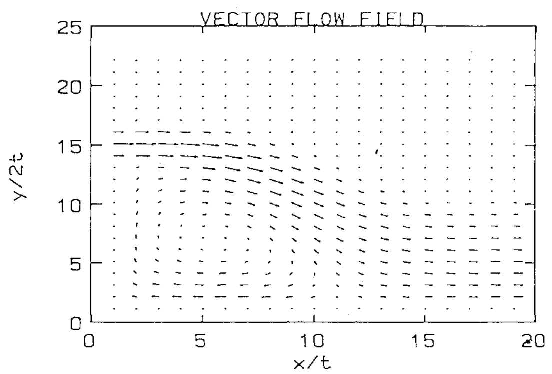

Fig. 3 Mean velocity vectors.

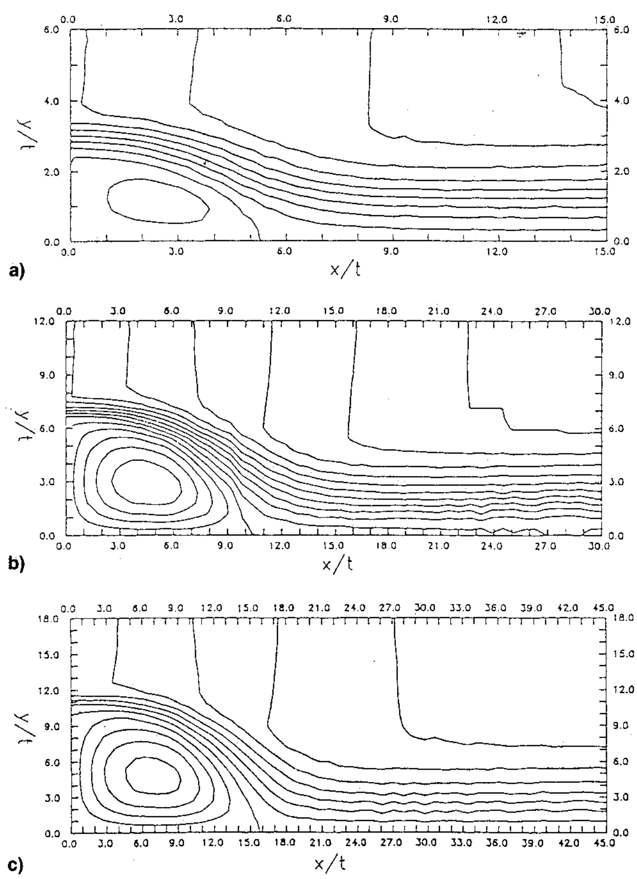

Fig. 4 Streamline of offset jet flow: a) *OR* = 3, b) *OR* = 7, and c) *OR* = 11.

54 grid lines in the cross-stream direction is enough. The solution is considered to be converged when the normalized residual of the algebraic equation is less than a prescribed value of 0.001.

IV. Results and Discussion

Figure 3 shows the mean velocity vectors of the flowfield with $OR = 7$. It is obvious that the flowfield can be divided into the recirculation region, the impingement region, and the wall jet region.

Figure 4 shows the streamline of the flowfield at different $OR = 3, 7, 11$. Referring to Fig. 4, in the case of large offset ratio, the corresponding streamline curvature of the jet centerline becomes large and the jet impinges to the flat plate nearly vertical.

V. Conclusions

Numerical solutions for turbulent offset jets that have been achieved by formulating the differential conservation equations governing the flow with an entrainment boundary requires large amounts of computer time in order to predict the finer details of the flow with sufficient resolution. Certain discrepancies between calculations and the available data may be caused by the isotropic assumption in the eddy viscosity/diffusivity model.

References

[1]Pelfrey, J. R. R., and Liburdy, J. A., "Mean Flow Characteristics of a Turbulent Offset Jet," *Journal of Fluids Engineering*, Vol. 108, No. 1, 1986, pp. 82–88.

[2]Pelfrey, J. R. R., "Characteristics of a Turbulent Plane Offset Jet," Ph.D. Dissertation, Mechanical Engineering Dept., Clemson Univ., Clemson, SC, 1984.

[3]Pelfrey, J. R. R., and Liburdy, J. A., "Effects of Curvature on the Turbulence of a Two-Dimensional Jet," *Experiment Fluids*, Vol. 4, No. 3, 1986, pp. 143–149.

[4]Bourque, C., and Newman, B. G., "Reattachment of a Two-Dimensional Incompressible Jet to an Adjacent Flat Plate," *Aeronaut Quar.*, Vol. 11, Aug. 1960, pp. 201–232.

[5]Sawyer, R. A., "The Flow Due to a Two-Dimensional Jet Issuing Parallel to a Flat Plate," *Journal of Fluid Mechanics*, Vol. 9, No. 4, 1960, pp. 543–560.

[6]Sawyer, R. A., "Two-Dimensional Reattachment Jet Flows Including the Effects of Curvature on Entrainment," *Journal of Fluid Mechanics*, Vol. 17, No. 4, 1963, pp. 481–498.

[7]Launder, B. E., and Spalding, D. B., "The Numerical Computation of Turbulent Flows," *Computer Methods in Applied Mechanics and Engineering*, Vol. 3, No. 2, 1974, pp. 269–289.

[8]Patankar, S. V., *Numerical Heat Transfer and Fluid Flow*, McGraw-Hill, New York, 1980, Chaps. 5 and 6, pp. 79–138.

Entrained Sprays from Meshed-Interface Occurring in a Heat Pipe

K. D. Kihm,* B. H. Kim,† and G. P. Peterson‡
Texas A&M University, College Station, Texas 77843

Nomenclature

L_1 = mesh length
L_2 = mesh height
Re_{L_1} = Reynolds number based on L_1

Received Nov. 19, 1992; revision received June 7, 1993; accepted for publication June 7, 1993.

*Assistant Professor of Mechanical Engineering. Member AIAA.

†Graduate Research Assistant.

‡Tenneco Professor and Head, Department of Mechanical Engineering. Associate Fellow AIAA.